The paper was presented at the Eleventh Meeting
"New Trends in Fatigue and Fracture" (NT2F11)
Polignano a Mare, Italy, 3–6 July, 2011

Vito Dattoma, Simone Giancane, Fania Palano, Francesco W. Panella

NON-DESTRUCTIVE SMALL DEFECTS DETECTION OF GFRP LAMINATES USING PULSED THERMOGRAPHY

OTKRIVANJE MALIH GREŠAKA BEZ RAZARANJA GFRP LAMINATA PRIMENOM IMPULSNE TERMOGRAFIJE

Originalni naučni rad / Original scientific paper
UDK /UDC: 620.179.13
Rad primljen / Paper received: 21.01.2012.

Adresa autora / Author's address:
Department of Engineering for Innovation, University of Salento, Lecce, Italy, email: vito.dattoma@unisalento.it

Keywords
- non-destructive testing
- GFRP (Glass Fiber Reinforced Polymer)
- pulsed thermography
- thermal contrast
- detection algorithm

Ključne reči
- ispitivanja bez razaranja
- GFRP (polimer ojačan staklenim vlaknima)
- impulsna termografija
- toplotni kontrast
- algoritam za detekciju

Abstract

This work explores the possibility to apply thermographic technique as a non destructive test to control glass fiber reinforced polymers having artificial defects.

Three symmetrical composite panels reinforced with fiberglass (unidirectional E type fiberglass and epoxy resin) are realized through hand lay-up and artificial inter-laminar delaminations of various geometry are introduced at different depths.

Several thermal stimulation procedures with different ways to consider the defects in the specimens enable to optimize the thermographic technique, by solving some initial problems related to the experimental set-up and issues. Above all, the minimum requirements for defect which can be revealed trough pulsed thermography have been established, according to present experiences. The importance of geometric and thermo-physic characteristics of the defect related to the material in which it is inserted has been observed, as well as the surface conditions of the observed laminate faces.

Izvod

U ovom radu je istražena mogućnost primene metode termografije, kao tehnika ispitivanja bez razaranja, za kontrolu polimera ojačanih staklenim vlaknima sa veštački unetim defektima.

Tri simetrične kompozitne ploče ojačane staklenim vlaknima (jednoosna staklena vlakna tipa E i epoksi smola) su pripremljene ručnim slaganjem i veštački su unete interlaminatne delaminacije različite geometrije, na različitim dubinama.

Nekoliko postupaka toplotne stimulacije sa različitim načinom razmatranja defekata u uzorcima omogućavaju optimizaciju termografske metode, rešavanjem nekih početnih problema vezanih za eksperimentalnu postavku i problematiku. Pre svega, ostvareni su minimalni zahtevi za defektom, koji se može otkriti impulsnom termografijom, a prema sadašnjim iskustvima. Razmatran je značaj geometrijskih i termo-fizičkih karakteristika defekta, povezanih sa materijalom u kojem je uveden, kao i uslovi površine posmatranih laminata.

INTRODUCTION

Thermography methods consist in the analysis of thermal emission spectrum in the infrared band. The attention is focused on the way in which a defect is able to produce a visible alteration of the thermal field in the surrounding material.

The work starts with the hand lay-up production of different GFRP panels in which the presence of the typical defects of this material have been artificially simulated. To investigate the presence of interlaminar delaminations, thin Teflon inserts or empty and filled holes suitably realized at specific depth have been realised.

A careful evaluation of the scientific literature has been necessary in order to preliminarily decide the configuration of the composite panels to be prepared (fibers orientation and laminate thickness) and the geometry of the defects to be artificially introduced. Furthermore, the bibliography is an useful starting point for the choice and the next optimisation of the thermographic parameters to be adopted for experimental analysis.

In the first ND experimental phase, two different GFRP panels (specimens 1 and 2) have been realized, to be tested through the Pulsed Thermography technique. Nevertheless, the need to improve the obtained results leads to the realization of another GFRP panel (specimen-panel 3), with the aim to optimize the characteristics of the inserted defect and testing procedures. The fundamental steps of this research work are:

– Hand lay-up production of 3 GFRP panels having inter-laminar delaminations artificially simulated inside; have been used thin Teflon inserts and drilled flat holes of different geometry and at specific depths;
– ND analysis by means of pulsed thermography of these composites with different procedures; in particular, tests with several heating times on specimens having defects with different dimensions and depth.
– Implementation of a Matlab tool in order to recognise defects from the acquired thermal images.

MATERIALS

Three symmetrical composite panels reinforced by incorporated fiberglass (unidirectional E type fiberglass and epoxy resin) are realized and artificial inter-laminar type small defects are introduced /1, 3, 4, 7/.

For the realization of the GFRP laminates, E glass fibers (density 600 g/m^2) organised in unidirectional coils (0°) and epoxy resin are used for symmetric multiple [0-90] stacking sequences. The characteristics and the codes of both materials are reported in the next table.

Table 1. Mechanical properties of glass fibers and epoxy resin.
Tabela 1. Mehaničke osobine staklenih vlakana i epoksi smole

E glass (prod. by Selcom Multiaxial Technology S.r.l.)	
Mean diameter (μm)	10
Young modulus (MPa)	73000
Ultimate stress (MPa)	3400
Ultimate strain (%)	4.8
Epoxy resin EC 130 LV + hardener W340 with ratio 100:37 (produced by Altana Varnish Compounds)	
Density (g/ml)	1.14–1.16
Young modulus (MPa)	2900–3100
Ultimate stress (MPa)	75–80
Ultimate strain (%)	8.5–9

The external surfaces of the panels have been made matte with a thin layer of black paint before the exposition to the thermal camera.

In laminate 1 (16 plies and approximate thickness 10 mm) defect geometry consists in blind circular holes up to 20 mm diameter with flat bottom and located at three different depths from the surface. The holes are about 1.5 mm deep.

In laminate 2 (20 plies and thickness 14 mm) thin Teflon folded inserts of thickness 0.2 mm, having circular and square shape of the same size, are introduced during lamination, at three different depths from the surface.

The laminate 3 (14 plies and thickness 7.5 mm) presents defects having greater dimensions respect to previous ones and particularly square empty holes in the middle ply, located at three different depths and having two different thicknesses; in order to increase the specimen thermal resistance, the laminates are painted with black varnish.

METHODS

Transient Thermography techniques analyse the cooling phase on component surface after it has been exposed to a short and intense thermal input. In the Pulsed Thermography the presence of defects and their characteristics are analysed by means of thermal contrast evaluation between sound zone and damaged areas /1, 7/ during the cooling phase.

The defects analysis is realized with a reflection set-up, the thermal camera and the light source on the same side, by means of a thermal camera FLIR 7500M and a thermal stimulation system formed by three or four 1000 W halogen lamps. The main parameters to be chosen for each test are the heating time t_{heat} and the observation period of the cooling phase t_{cool}. Other variables are the acquisition frequency of the images, the integration time and the number of images to be acquired.

FLIR 7500M model thermal camera has a detector FPA in InSb sensors, cooled through Stirling cycle and has the following technical characteristics:

– image size 320 × 256 pixel
– thermal resolution < 25 mK and precision ±1%
– integration time 3–20 000 μs

The software employed are Cirrus for internal configuration of thermal camera management and Altair only for acquisition of the images.

The pulsed thermography analysis could present some limits such as needed to preliminarily know the sound areas of the material and dependence of thermal contrast from the sound zone choice; the ideal condition for thermal contrast calculation is verified when the sound area is ensured to receive the same heat flux of the defected one and the incident heat flux reaches the defect only after the lamps turn off.

The post processing analysis is structured in the following steps:

1. Thermal image and map of isotherm curves at the beginning of the transient cooling.
2. Choice of the reference frame.
3. Selection of 2 rectangular areas with represents, respectively, the defect and the sound zones.
4. Calculation of the mean temperature for the two zones and determination of the thermal contrast.
5. Estimation of the inversion time during the cooling phase.
6. Analysis and trend search of defect thermal contrast with respect to sound reference area.

RESULTS

The frames sequence are exported in ASCII format, in order to manage it with the software MATLAB for the realization of personalised post-processing data. The algorithm is endowed with an interactive interface, which allows the user to make geometrical and in-time choices or to specify some analysis parameters.

The algorithm gives the temperature trends, referred to the sound and the defected areas, during all the acquisition time and shows also the instant in which the defect temperature is the same of the reference one (inversion time). Subsequently the routine provides diagrams obtained during the transient cooling for the normalised thermal contrast C_n (a-dimensional) and the absolute one C_a; these parameters allows to achieve more reliable comparison between different defects and the reference points. For both the thermal contrast definitions, the algorithm computes two quantitative parameters connected to the defect characteristics (depth and size): the maximum value of contrast $C_{\max}$ and the observation time $t_{\max}$, the period between the lamps turning off and the instant of maximum measured contrast /1, 3, 4, 7/.

The analysis on specimens 1 and 2 is realized with a reflection thermographic set-up, with the light source and the thermal camera from the same side, and the simultaneously turning-on of three 1000 W halogen lamps, located at a distance of 1 m from the specimen (Fig. 1) at specific and optimised angles.

Figure 1. Thermographic set-up for specimens 1 and 2.
Slika 1. Termografska priprema za uzorke 1 i 2

For what concerns specimen 1, no test is allowed to identify any defect. The thickness of teflon layers and air spaces are too thin to be revealed with PT technique for this kind of material.

For specimen 2, only defects having diameters between 4 and 12 mm, located at depth 2.5 mm, can be highlighted and they were already visible during the transient cooling (pre-heat storage). The PT technique in the specimen 1 analysis was not successful, probably due to defect characteristics: the thickness of Teflon and the air spaces were too small and also because the material is particularly not inside due to the presence of the composite layers and superficial condition not perfectly constant. This resulted in the presence of elevated thermal scatter of the measured temperatures in time, which did not allow to detect significant temperature differences below a certain level. In the specimen 2, despite the preheating phenomena in the defected zone, the presence of some sub-superficial defects having diameters between 4 and 8 mm was obtained; in fact, for each defect $C_{a\,\max}$ showed to rise in a quadratic way when the heating time increases; the problem of the heat storage on defects can be solved by limiting the time of thermal exposition.

If geometrical and thermo-physical properties of the defects are inadequate to be revealed by thermography it is appropriate to adopt greater holes filled only with air or use different ND procedures.

When the thermal map is not uniform, the reason could be the presence of reflections due to hot sources or by material characteristics, such as manufacturing superficial imperfections or the uncorrected disposition of light sources. These problems can be reduced if the specimen is painted with matt black paint and with the adoption of an experimental procedure for the optimisation of the thermographic set-up.

The optimal experimental set-up includes the simultaneous lighting of 4 halogen 1000 W lamps, located at a 75 cm distance from the specimen and angled more then in the previous tests, and the thermal camera at a distance of 1 m (Fig. 2).

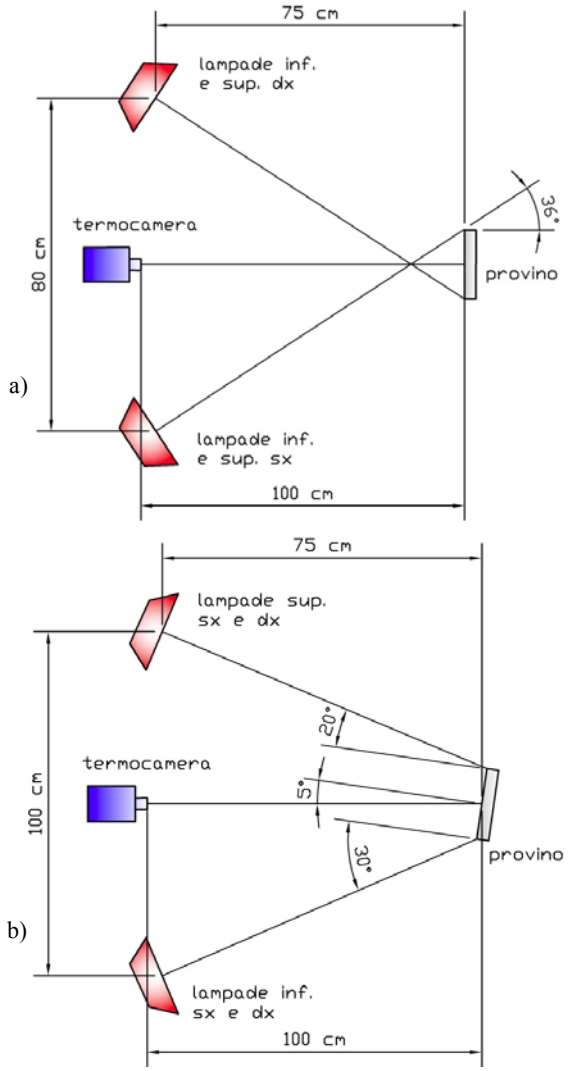

Figure 2. Top view a) and lateral view b) of the thermographic set-up for specimen 3.

Slika 2. Pogled odozgo a) i sa strane b) termografske pripreme za uzorak 3

For specimen 3, a very short heating time is adopted to avoid the pre-heating phenomena and the distance, and the orientation of the lamps was improved to reduce the heat distribution non-uniformity.

Both surfaces of the specimen are observed in order to examine imperfections having the same dimensions at three different depths: 1, 2 and 4.5 mm. Several heating times are considered in order to establish the minimum dimension and the maximum depth of the defects that can be revealed in specimen 3.

The experimental plan is illustrated in Table 2, where the heating time and the acquisition time values are reported.

Artificial defects are marked with progressive numbers from 1 to 8. The geometric characteristic of the defects are resumed in Table 3.

Table 2. Tests planning for specimen 3.
Tabela 2. Ispitivanje uzorka 3

Test number	Observed surface	t_{heat} (s)	t_{acq} (s)
1	front	2	242
2	front	5	365
3	front	10	490
4	front	20	620
5	back	5	365
6	back	10	490
7	back	20	620
8	back	30	750

Table 3. Geometric characteristics of the defects for specimen 3.
Tabela 3. Geometrijske karakteristike defekata za uzorak 3

Defect number	1	2	3	4	5	6	7	8
dimension (mm)	40	30	20	10	40	30	20	10
depth (mm)	1	1	1	1	2	2	2	2
thickness (mm)	2	2	2	2	1	1	1	1

Figure 3. Thermographic set-up for specimen 3.
Slika 3. Termografska priprema za uzorak 3

A heating time of 2 seconds is sufficient to detect all the 8 defects located in the panel.

A short thermal stimulation allows to adequately limit the appearance of heat storage in the defects. So, the thermal map and the isothermal plot (Fig. 4), recorded at the beginning of the cooling phase, do not present hot points, even if the heating of the specimen is not perfectly uniform.

In Figure 4, the thermal map after 35 s of the cooling step is reported in particular.

The post processing phase of the thermal images allows to study each defect, highlight their main characteristics. In the following images the complete analysis for the defect 1 is presented as an example, which is the larger sub-superficial defect (width 40 mm, depth 1 mm). The presence of an air space reduces the heat transmission of the material so that, by observing the superficial temperature, the defect appears like an area hotter than the sound one. At the end of the cooling phase the temperatures of both areas become equal.

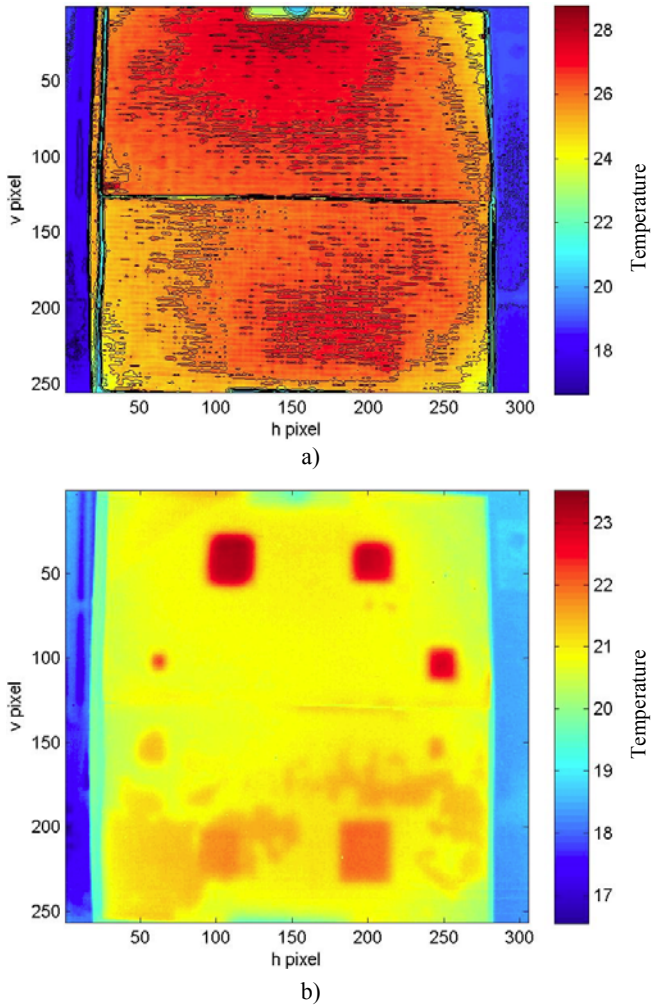

Figure 4. a) Map of isothermal curves acquired at the beginning of the cooling phase (heating for 2 s); b) thermal image recorded 35 s after the lamps turning off (heating for 2 s).
Slika 4. a) Mapa iizotermi dobijenih na početku faze hlađenja (zagrevanje za 2 s); b) termalna slika snimljena 35 s posle isključenja lampe (zagrevanje za 2 s)

The trends of the normalised thermal contrast and the absolute one, during the transient cooling, are illustrated in Fig. 5. The normalised contrast curve is regular, but it presents some anomalies in the final part, in which it assumes little negative values. From the curve of the absolute contrast, an initial pre-heating storage of about 0.5°C for the defect is evident.

Both the curves reach a maximum value C_{max} after 21 s from the lights turning off. In this instant t_{max}, the imperfection shows a pronounced thermal profile, which makes it easily to distinguish with respect to the surrounding sound area.

Figure 6 reproduces the real profile of the defect, despite the presence of a noisy thermal signal, which shows the theoretical "cup" trend of a defect observed in reflection. In this condition the maximum value of the absolute thermal contrast $C_{a\,max}$ is equal to about 2.4°C.

The extension of the heating duration from 2 to 20 s allows to increase the thermal contrast for each imperfection, but it determines a pre-heating storage in all the defects. Figure 7 shows the thermal image recorded at the beginning of the transient cooling. A pre-heating storage is marked for all the defects: this problem can be solved through a suitable choice of the sound area.

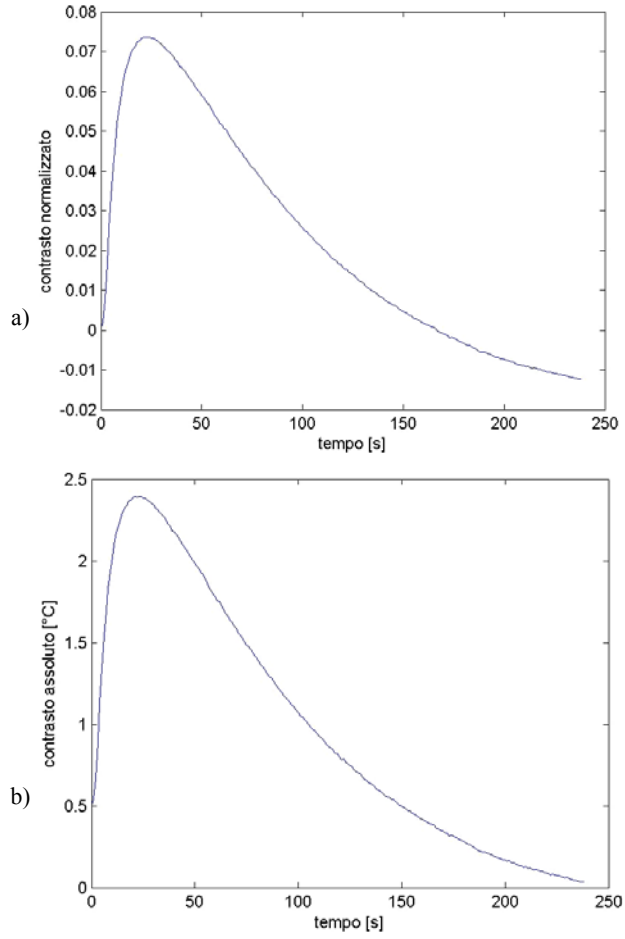

Figure 5. Trends of the normalised contrast a), and absolute b), for defect 1 during the transient of cooling (heating for 2 s).
Slika 5. Promene u normalizovanom a), i u apsolutnom b) kontrastu, za defekt 1 tokom hlađenja (zagrevanje za 2 s)

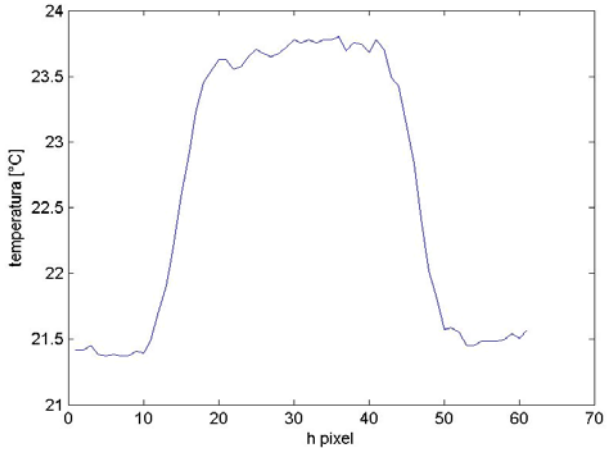

Figure 6. Thermal profile for defects 1, acquired 21 s after the lamps turning off (heating for 2 s).
Slika 6. Toplotni profil za defekte 1, dobijen 21 s posle isključenja lampe (zagrevanje za 2 s)

The thermal image after 30 s from the lamps turning off, reported in Fig. 7b, consents to clearly distinguish all the defects. In Fig. 8 there is the diagram during the whole acquisition of temperature versus time recorded for defect 1 and the related sound zone.

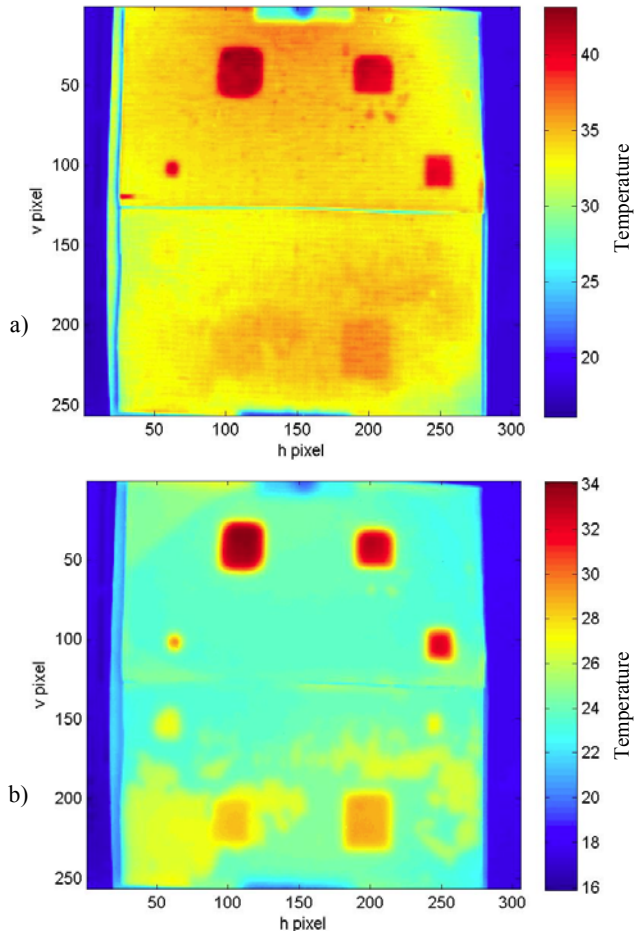

Figure 7. a) Thermal image recorded at the beginning of the transient of cooling and b) after 30 s from the lamps turning off (heating for 2 s).
Slika 7. a) Toplotna slika dobijena na početku hlađenja i b) posle 30 s od isključenja lampe (zagrevanje za 2 s)

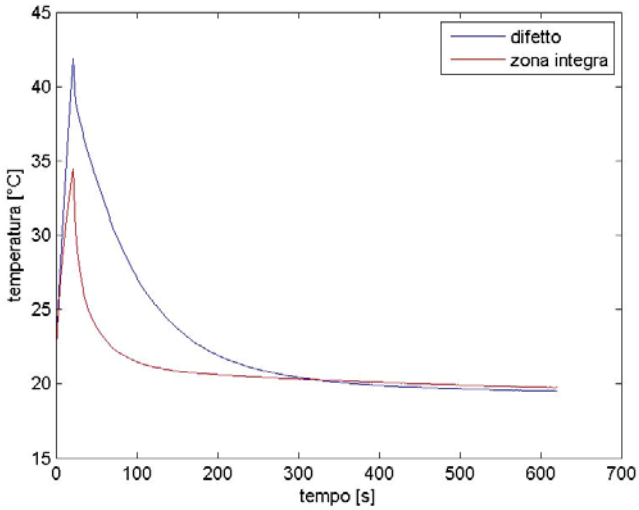

Figure 8. Temperature change in time for defect 1 and integration zone (heating for 20 s).
Slika 8. Promena temperature sa vremenom za defekt 1 i zonu integracije (zagrevanje za 20 s)

The previous figure enables to identify a particular time instant (inversion time) equal to 299 s after which the defect appears no longer as a hot point, but as cold one. This involves that the absolute thermal contrast assumes negative values for $t > t_{inv}$. Figure 9 shows the thermal image acquired 380 s after the lamps turning off: all the sub-superficial imperfections (located in the upper half of the specimen, at depth 1 mm) have reached their characteristic inversion time and they appear as cold points.

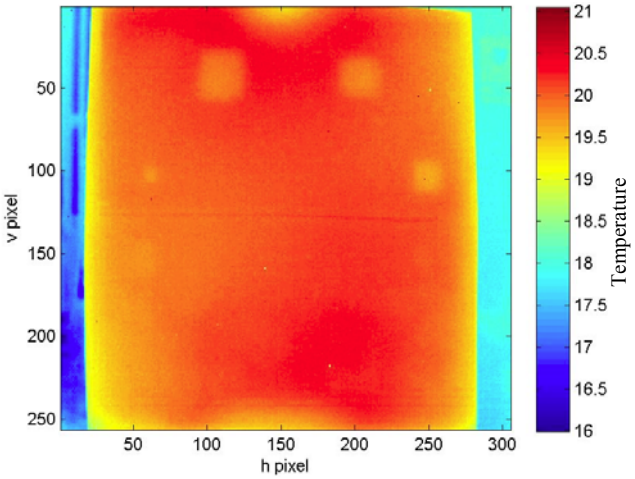

Figure 9. Thermal image acquired 380 s after the lamps turning off (heating for 20 s)
Slika 9. Toplotna slika dobijena posle 380 s od isključenja lampe (zagrevanje za 20 s)

As previously affirmed, the specimen has been observed by directing the thermal camera before towards the front surface (tests 1–4) and then the back surface (tests 5–8) of the specimen. When the rear panel surface is observed, a heating time of 5 s is sufficient to recognise all 8 defects. The depth of 4.5 mm is able to guarantee the absence of pre-heating storage even if the thermal stimulation is long (t_{rheat} till 30 s in test 8).

In Figure 10, the trends of maximum absolute contrast $C_{a\,\max}$ and observation time $t_{a\,\max}$ versus the thermal stimulation time t_{ris} are illustrated for defects 1–8 (located at depths 1 and 2 mm).

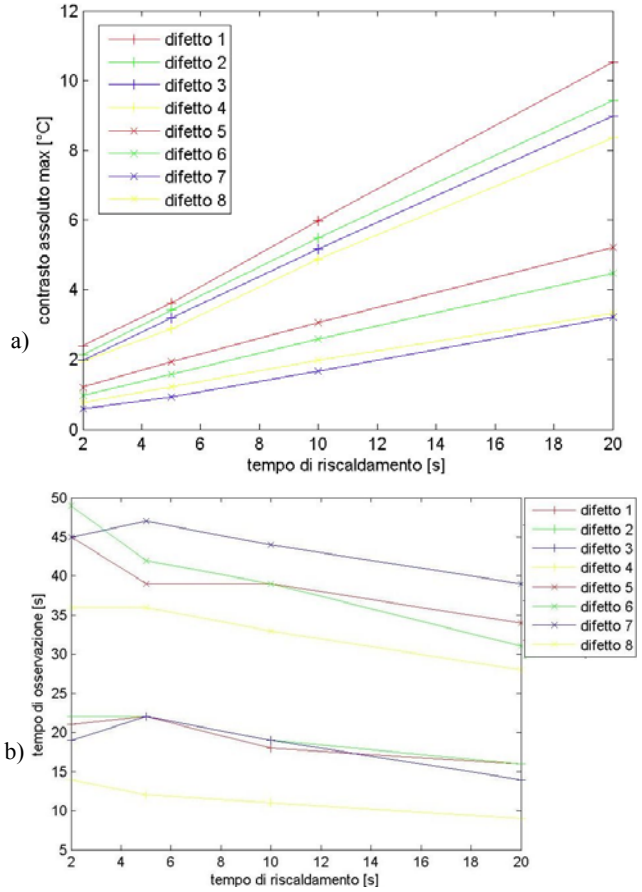

Figure 10. Absolute contrast to maximum a) and the observation time b) as a function of heating duration, for defects 1–8.
Slika 10. Apsolutni kontrast do maksimalnog a) i vreme posmatranja b) u funkciji zagrevanja, za defekte 1–8

$C_{a\,\max}$ linearly increases, while $t_{a\,\max}$ decreases when t_{ris} arises. Each defect is visible before and with a greater thermal contrast if the heating time is longer. Regarding the geometrical characteristics of the defects, $C_{a\,\max}$ diminishes while $t_{a\,\max}$ rises when depth and dimensions increase.

The same comparison for $C_{a\,\max}$ and $t_{a\,\max}$ versus t_{ris} could be realized for imperfections observed from the back surface of the panel (at depth of 4.5 mm), so to reveal the possible influence of the defect thickness on these parameters, if the defect depth is the same.

In Figure 11, the variation of $C_{a\,\max}$ in respect to dimensions and depth of imperfections is showed. The parameter that influences more the $C_{a\,\max}$ is the deepness of the defect, while its dimensions seem to be less influent. Particularly, if the imperfection is located at a depth greater than 5 mm, $C_{a\,\max}$ becomes lower than 1 and so it is difficult to be identify.

In Figure 12, $t_{a\,\max}$ variation in respect to the dimension and the deepness of the defect is reported. Also in this situation, the influence of depth is clear, but there is no evidence of any dependence from dimension.

In Figure 13 inversion time as function of dimensions of defect, for several heating times, is reported. Generally, t_{inv} arises with t_{heat}: this signifies that greater the heat gain, greater is the time the imperfection becomes thermally uniform with the sound area.

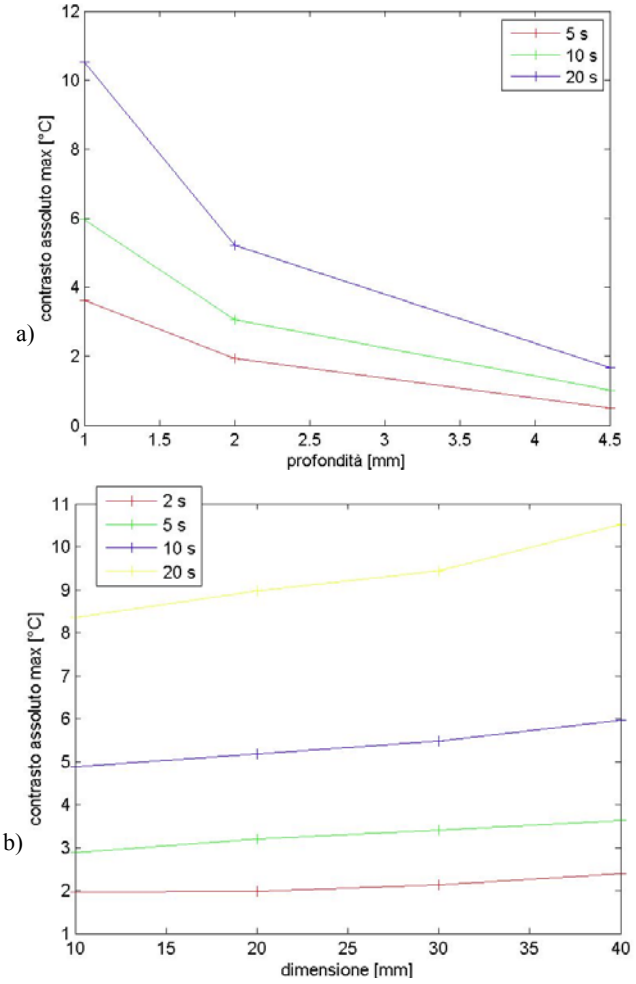

Figure 11. Trend of absolute contrast to maximum as a function of defect size, for different heating times at the same depth (defects 1–4) (a), and trend of absolute contrast to maximum as a function of defect depth, for different heating times at equal size defects, (1, 5, 1_{bis}) (b).
Slika 11. Promena apsolutnog kontrasta do maksimalnog u funkciji veličine defekta, za različita vremena zagrevanja na istoj dubini (defekti 1–4) (a), i promena apsolutnog kontrasta do maksimalnog u funkciji dubine defekta, za različita vremena zagrevanja za defekte iste veličine, (1, 5, 1_{bis}) (b)

Few data obtained allow to note that an increase of t_{inv} when the depth of the imperfection rises; probably, a more deep defect needs longer time not only to be identified, but also to become thermally uniform with the sound zone.

CONCLUSIONS

Research activities have allowed to gain the aim to characterize in an exhaustive manner the pulsed thermographic technique for non-destructive control of GFRP composites.

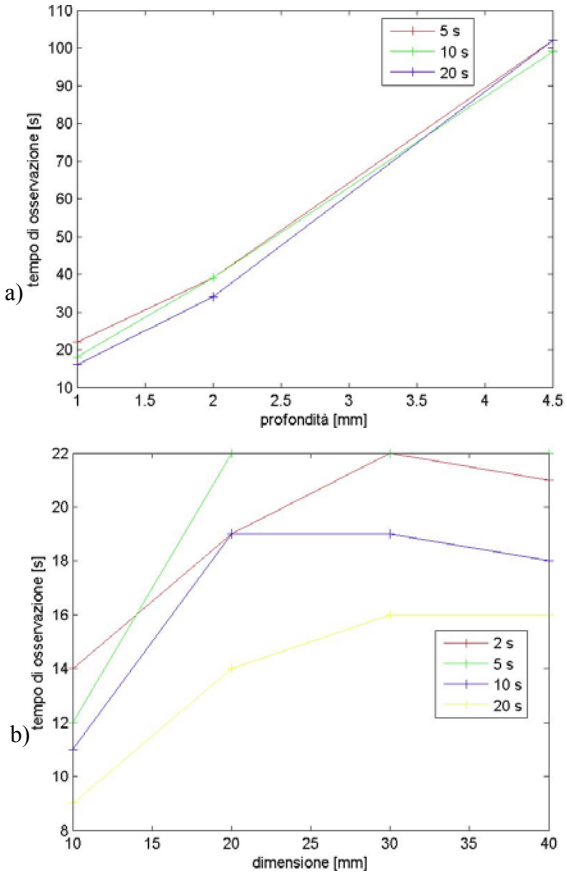

Figure 12. Trend of time as a function of defect size, for different heating times at the same depth (defects 1–4) (a), and trend of time as a function of defect depth, for different heating times at equal size defects, (1, 5, 1_{bis}) (b).

Slika 12. Promena vremena u funkciji veličine defekta, za različita vremena zagrevanja na istoj dubini (defekti 1–4) (a), i promena vremena u funkciji dubine defekta, za različita vremena zagrevanja za defekte iste veličine, (1, 5, 1_{bis}) (b)

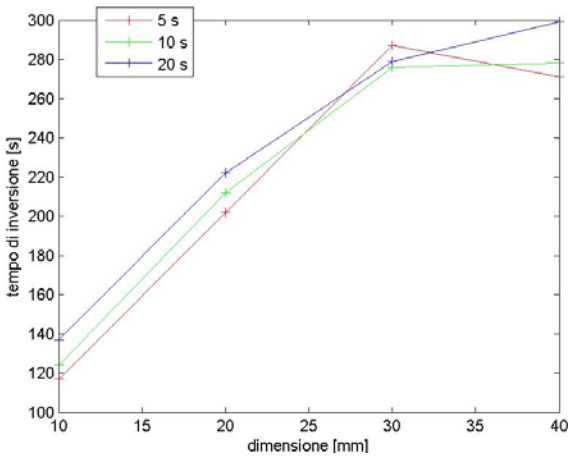

Figure 13. Trend of inversion time versus defect dimensions for several heating times, (defects 1–4 at the same depth).

Slika 13. Promena inverznog vremena prema veličini defekata za nekoliko vremena zagrevanja, (defekti 1–4 na istoj dubini)

Several tests of thermal stimulation and different ways to simulate defects in specimens enable to optimise the thermographic technique by solving some initial problems related to the experimental set-up. Above all, the minimal requirements are established, so that an artificial defect can be revealed through pulsed thermography. The importance of geometrical and thermo-physical characteristics of the defect related to the material in which it is inserted is highlighted. Particularly, the adopted processes allowed to identify air spaces up to a maximal depth of 4.5 mm, having minimal thickness 1 mm and minimal width of 10 mm.

Furthermore, the initial problems of pre-heat storage in the defect and dis-uniformity of the thermal map are faced and solved, establishing the optimal parameters for the realisation of the thermographic analysis.

Better results are obtained when four 1000 W halogen lamps are lit. The lamps are located at a distance from the specimen of 75 cm and suitably oriented towards the vertex of the panel, so that the angle of attack is greater than the angle of observation of the thermal camera. The infrared scanner, instead, is positioned behind the lamps array, at 1 m from the specimen.

Particularly, heating for 2 s is sufficient to identify defects having 2 mm depth and thickness 1 mm, while heating of 5 s is necessary to identify imperfections having depth 4.5 mm and thickness of 1 mm. The heat gain in both situations is able to limit the pre-heat storage effect in the defect. Finally, the influence of the thermal pulse and the geometrical characteristics of the defect on several experimental parameters, such as the maximal absolute contrast $C_{a\ max}$, the observation time $t_{a\ max}$ and the inversion time t_{inv} is evaluated.

If the heating time is extended, each defect is visible before and with a greater thermal contrast. The parameter that mostly influences $C_{a\ max}$ and $t_{a\ max}$ is the depth. If the depth diminishes, the defect is visible before and with a greater thermal contrast. Generally, the inversion time t_{inv} increases when the pulse time and the depth of the defect increases. A clear rise of the C_a parameter when the defect dimension increases and its depth diminishes, can be noticed; moreover, the inversion time rises if the size and depth of defects increase.

REFERENCES

1. Giorleo, G., Meola, C., *Location and geometry of defects in composite laminates from infrared images*, Journal of Materials Engineering and Performance, Vol.7(3), June 1998, pp.367--374.
2. Dattoma, V., Marcuccio, R., Pappalettere, C., Smith, G.M., *Thermographic investigation of sandwich structure made of composite material*, NDT&E International, Vol.34, 2001, pp.515-520.
3. Avdelidis, N.P., Hawtin, B.C., Almond, D.P., *Transient thermography in the assessment of defects of aircraft composites*, NDT & E International, Vol.36, 2003, pp.433-439.
4. Meola, C., Carlomagno, G.M., Giorleo, L., *Geometrical limitations to detection of defects in composites by means of infrared thermography*, Journal of Nondestructive Evaluation, Vol.23, No.4, December 2004, pp.125-132.
5. Dudzik, S., *A simple method for defect area detection using active thermography*, Opto-Electronics Rev, Vol.17 (4), 2009, pp.338-344.
6. Pitarresi, G., Riforgiato, F., *Implementazione di tecniche NDT di termografia ad infrarossi su pannelli in composito GRP per applicazioni nautiche*, XXXIX AIAS Congress AIAS, 7-10 September 2010, Maratea, Italy.
7. Maldague, X., Galmiche, F., Ziadi, A., *Advances in pulsed phase thermography*, Infrared Physics & Technology, Vol.43, 2002, pp.175-181.